Identification of non-mutated neoantigens presented by TAP-deficient tumors

Marijt, K.A.; Blijleven, L.; Verdegaal, E.M.E.; Kester, M.G.; Kowalewski, D.J.; Rammensee, H.G.; ... ; Hall, T. van

JEM Journal of Experimental Medicine

ARTICLE

Identification of non-mutated neoantigens presented by TAP-deficient tumors

Koen A. Marijt[1], Laura Blijleven[1], Els M.E. Verdegaal[1], Michel G. Kester[2], Daniel J. Kowalewski[3,4], Hans-Georg Rammensee[3,4], Stefan Stevanović[3,4], Mirjam H.M. Heemskerk[2], Sjoerd H. van der Burg[1], and Thorbald van Hall[1]

Most T cell–based immunotherapies of cancer depend on intact antigen presentation by HLA class I molecules (HLA-I). However, defects in the antigen-processing machinery can cause downregulation of HLA-I, rendering tumor cells resistant to CD8$^+$ T cells. Previously, we demonstrated that a unique category of cancer antigens is selectively presented by tumor cells deficient for the peptide transporter TAP, enabling a specific attack of such tumors without causing immunopathology in mouse models. With a novel combinatorial screening approach, we now identify 16 antigens of this category in humans. These HLA-A*02:01 presented peptides do not derive from the mutanome of cancers, but are of "self" origin and therefore constitute universal neoantigens. Indeed, CD8$^+$ T cells specific for the leader peptide of the ubiquitously expressed LRP AP1 protein recognized TAP-deficient, HLA-I^{low} lymphomas, melanomas, and renal and colon carcinomas, but not healthy counterparts. In contrast to personalized mutanome-targeted therapies, these conserved neoantigens and their cognate receptors can be exploited for immune-escaped cancers across diverse histological origins.

Introduction

Many T cell–based immunotherapies for cancer are based on recognition of tumor antigens presented in HLA class I (HLA-I) molecules by tumor cells (Robbins et al., 2013; Schumacher and Schreiber, 2015). Success of immune checkpoint blockade therapy is strongly correlated with mutational load and mismatch repair-deficient cancers, irrespective of tumor type (Snyder et al., 2014; Lauss et al., 2017). Point-mutated peptides indeed constitute formidable tumor antigens due to their nonself nature, for which a noncurtailed T cell repertoire is available. An absolute requirement for such T cells to exert their action against cancer is the display of HLA-I at the surface of tumor cells. However, HLA-I down-modulation on cancer cells is observed in many immune-escaped cancers, often caused by epigenetic silencing of antigen-processing components, like the transporter associated with antigen processing (TAP; Setiadi et al., 2007; Garrido et al., 2016; Ritter et al., 2017). Recent studies implicated that acquired resistance to checkpoint therapy can occur through alterations in genes relevant for antigen processing and presentation (Patel et al., 2017; Sucker et al., 2017). For instance, mutations in the JAK1/JAK2 IFN signaling pathway represented acquired and primary resistance mechanisms in cancer patients who relapsed from or did not respond at all to checkpoint therapy, respectively. Notably, these mutations resulted in the inability to respond to IFN-γ and thus to upregulate antigen processing and presentation by HLA-I (Gao et al., 2016; Zaretsky et al., 2016; Shin et al., 2017).

Our group previously discovered a novel category of tumor antigens, referred to as TEIPP (T cell epitopes associated with peptide processing), that are presented at the surface of tumor cells carrying defects in antigen processing (Marijt et al., 2018). In mouse tumor models in which MHC-I display is down-modulated by defects in the peptide transporter TAP, we showed a selective presentation of TEIPP peptides and successful targeting of immune-escaped tumor variants by TEIPP-specific T cells (Doorduijn et al., 2016, 2018a). Thus, targeting TEIPP neoantigens is a potent strategy to induce antitumor responses for tumors with low MHC-I expression. TEIPPs are derived from ubiquitously expressed non-mutated "self" proteins; however, their processed peptides fail to be loaded into MHC-I in healthy cells. Their surface presentation is highly promoted by defects in the antigen-processing machinery, especially in the absence of the peptide transporter TAP. Due to this virtue, TEIPP peptides constitute tumor-specific antigens. We have shown that the CD8$^+$ T cell repertoire against TEIPP neoantigens is positively selected in the thymus and that these cells remain naive, even in tumor-bearing mice, making this subset fully exploitable for T cell–based therapies against immune-escaped cancers without

[1]Department of Medical Oncology, Leiden University Medical Center, Leiden, Netherlands; [2]Department of Hematology, Leiden University Medical Center, Leiden, Netherlands; [3]Department of Immunology, Institute for Cell Biology, University of Tübingen, Tübingen, Germany; [4]German Cancer Consortium, German Cancer Research Center, Tübingen, Germany.

Correspondence to Thorbald van Hall: T.van_Hall@lumc.nl.

any signs of autoimmune reactivity (Doorduijn et al., 2018a). As of yet, only one human TEIPP neoantigen has been identified at the molecular level (El Hage et al., 2008; Durgeau et al., 2011).

To identify multiple human TEIPP antigens, we developed a systematic hybrid forward-reversed immunology screen to identify human TEIPP antigens. This approach encompassed an in silico prediction of TEIPP neoantigen candidates from the whole humane proteome, matching candidates to the cancer-specific peptidome, and an ex vivo screen to confirm the presence of a TEIPP T cell repertoire in healthy donors. Here, we present data on 16 identified HLA-A*02:01–binding TEIPP epitopes and a full characterization of the T cell reactivity against one of them.

Results

Strategy for target identification from the complete human proteome

To identify human TEIPP antigens that are presented by TAP-deficient cancer cells, we developed a hybrid forward-reversed immunology identification approach based on alternative antigen-processing rules in combination with cancer-specific peptidome database matching (Fig. 1 A). The whole human proteome was chosen as a starting point, since TEIPP antigens are non-mutated self antigens that are preferentially displayed on cells with deficiency in the peptide transporter TAP. This TAP-independent loading in HLA-I molecules can occur via two known alternative processing pathways: liberation of N-terminal "signal peptides" and C-terminal "tail peptides" (Martoglio and Dobberstein, 1998; Yewdell et al., 1998; Neefjes et al., 2011; Blum et al., 2013; Oliveira et al., 2013; Fig. 1, A and B). A list of signal peptide–containing proteins was selected from the human proteome with the use of a web-based algorithm that predicts the signal peptidase cleavage site (Käll et al., 2004). Most of these leader peptides need further processing by the proteolytic enzyme signal peptide peptidase in order to release them from the ER membrane and thereby generate peptides of different lengths suitable for loading in HLA-I (Martoglio and Dobberstein, 1998; Blum et al., 2013). This signal peptide search yielded 111,525 different 9- and 10-mer TEIPP candidates. Additionally, C-terminal tail peptides were selected using information on the topology of transmembrane proteins in the same web-based algorithm, knowing that liberation and TAP-independent processing of C-termini can be exerted by proteases like furin and signal peptide peptidase (Tiwari et al., 2007; Medina et al., 2009; Leonhardt et al., 2010, 2011; Oliveira et al., 2013). This search resulted in 6,674 tail peptides (Fig. 1, A and B). Next, we filtered these combined peptides for a predicted high HLA-I binding affinity (IC50 < 500 nM) to one of the so-called HLA "supertypes," representing most alleles in the Caucasian population (HLA-A*01:01, HLA-A*02:01, HLA-A*03:01, HLA-B*07:02, HLA-B*40:01, and HLA-A*24:02; Sette and Sidney, 1999; Nielsen et al., 2003; Sidney et al., 2008; Andreatta and Nielsen, 2016). This final list of 13,731 TEIPP candidates was then cross-matched with a large peptidome database containing peptides eluted from >200 tumor samples and 120 healthy tissue control samples (Table S1). Thereby, we focused on those TEIPP candidates that were endogenously processed and exclusively presented by tumor cells (Fig. 1 C). This strategy yielded a short list of 65 TEIPP neoantigen candidates, of which 40 had a predicted binding to the HLA-A*02:01 allele (Fig. S1, A–D). These 40 HLA-A*02:01–binding peptides were chosen to explore the existence of cognate CD8+ T cells (Fig. 1 A).

Detectable frequencies of CD8+ T cells against 16 out of 40 HLA-A*02:01–binding TEIPP neoantigens

To validate that T cells against these TEIPP neoantigens were present in the repertoire of healthy donors, we grouped 40 different HLA-A*02:01 tetramers containing the TEIPP neoantigens in eight pools of five peptides each, based on predicted binding affinity (from high in "peptide pool 1" to low in "peptide pool 8"). Next, CD8+ T cell cultures were started with tetramer-assisted "pull-downs" from peripheral blood mononuclear cells (PBMCs). These enriched CD8+ T cell pools were stimulated with the five respective synthetic peptides of that particular pool for several rounds and analyzed for the presence of peptide-specific T cells by flow cytometry (Fig. 2 A). In an initial screen of three different HLA-A*02:01–positive healthy donors, we observed T cell repertoires for 16 out of 40 TEIPP neoantigen candidates (Fig. 2 A). Frequencies of tetramer-stained CD8+ T cells varied from 0.1% up to 78% in these short-term expanded cultures. These percentages differed between the three tested donors, indicating that this protocol enabled the detection of TEIPP-specific CD8+ T cells, but that the observed frequencies reflected variation of the in vitro steps of enrichment and expansion. Additional donors were examined for the 16 positive peptides to evaluate the consistency of this finding, and, against most peptides, CD8+ T cells were detected in the majority of the donors (Fig. 2 B and Table 1). Collectively, these data indicated that our TEIPP identification strategy had a high success rate to identify human antigens in which a CD8+ T cell repertoire existed in healthy individuals.

Most TEIPP-specific CD8+ T cells reside in the naive repertoire

Previous investigations in our mouse tumor model of TEIPP showed that TEIPP-specific T cells remain naive, even in the presence of TAP-deficient tumor cells (Doorduijn et al., 2018a). This was shown to be an advantage for their exploitability in therapeutic interventions (Doorduijn et al., 2018a). To test this aspect for human TEIPP-specific T cells, we again enriched tetramer-positive CD8+ T cells from PBMCs for the five peptides (p14, p29, p34, p35, and p55) that were frequently positive in our screen. Naive CD8+ T cells were directly separated from antigen-experienced CD8+ T cells by flow cytometry sorting, based on differentiation markers CD62L and CD45RA at the cell surface (Fig. S2 A). After this ex vivo sorting, the two populations were expanded by three rounds of in vitro stimulation and analyzed for the presence of tetramer-positive CD8+ T cells (Fig. 3, A and B). Importantly, T cells against p14, p34, and p35 were exclusively found in the sorted naive population in all tested donors, indicating that these specificities had never encountered cognate antigen in these healthy individuals. In addition, T cells against p29 and p55 were found in the naive subset of some donors, while in other donors, these specificities were detected in the antigen-experienced repertoire (Fig. 3 B). These data indicated that some TEIPP-specific CD8+ T cells already had been primed in a few healthy individuals, but that the majority of them reside in

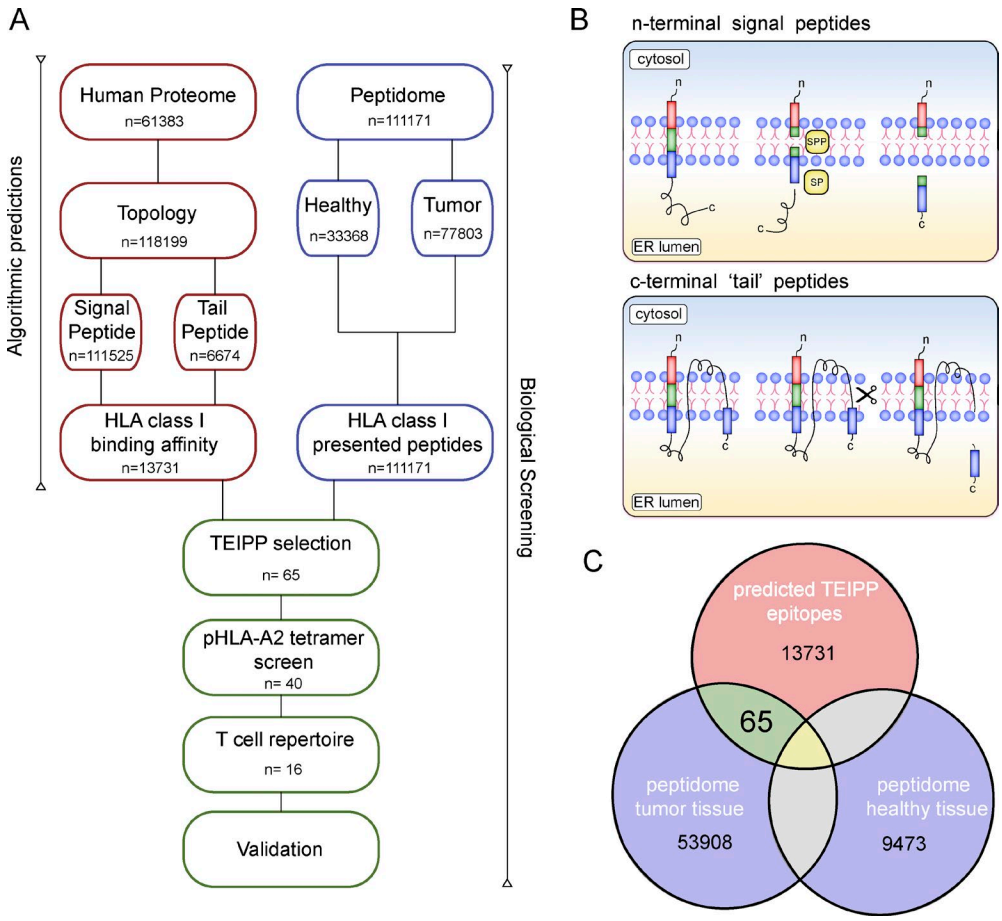

Figure 1. **Identification approach of TEIPP neoantigens associated with immune-edited cancers. (A)** A schematic overview of the applied screening approach. Human peptide sequences were selected via algorithms-based predictions on the whole human proteome for presentation by HLA-I molecules independent of the peptide transporter TAP. Two main unraveled pathways have been described for which algorithms are available: the processing of signal peptides and of C-terminal tail peptides (red). The resulting peptide selection was matched with a large database of naturally presented peptides from human cancers and healthy tissue (blue). The subsequent short list of candidates with a predicted binding to HLA-A*02:01 was subjected to functional testing for T cell immunogenicity and recognition of tumor cells deficient for the peptide transporter (green). **(B)** Graphical display of the two molecularly described TAP-independent processing mechanisms. Top: Signal peptides containing proteins are processed in the ER membrane by the proteolytic enzymes signal peptidase (SP) and signal peptide peptidase (SPP), resulting in the liberation of small peptides in the lumen of the ER, where they can bind to HLA-I molecules. Bottom: Proteins with their C-terminal tail protruding in the ER can be cleaved by proteases like furins or single peptide peptidase. **(C)** Venn diagram of in silico predicted TEIPP neoantigens matched with databases comprising naturally presented peptides from tumor tissues or healthy tissues.

a naive state. We speculated that this priming could have been triggered by bacterial species in the gut with antigens that show striking sequence similarity with peptide 29 and 55 (Fig. S2 B). In summary, these data demonstrate a universal existence of naive T cells with TEIPP specificity in healthy individuals.

Functional avidity of clonal CD8⁺ T cell cultures

To functionally study TEIPP-specific CD8⁺ T cells, we generated clonal cultures against the five TEIPP peptides p14, p29, p34, p35, and p55. Four of these peptides were derived from N-terminal signal sequences of proteins, and one was derived from a C-terminal tail peptide (Fig. S2 C). We evaluated the binding affinity and stability of these five peptides to HLA-A*02:01 since these determinants are critically involved in immunogenicity for T cells (van der Burg et al., 1996; Müllbacher et al., 1999). Four of the five peptides displayed an intermediate affinity and formed complexes with HLA-A*02:01 for at least 4 h; however, p29 surprisingly failed to show binding in these cellular assays (Fig. S2, D and E). Multiple T cell clones were generated using an antigen-independent expansion protocol of tetramer-positive CD8⁺ T cells after single-cell sorting. Since the functional avidity correlates with high affinity TCRs and thus for in vivo efficacy (Dutoit et al., 2001; Snyder et al., 2003; McKee et al., 2005; Viganò et al., 2012), we assessed the peptide concentrations resulting in half-maximum cytokine response (EC50) of the several TEIPP-specific T cell clones when exposed to APCs pulsed with titrated concentrations of cognate peptide (Fig. 3 C). All isolated T cell clones exhibited a functional avidity between 0.4 and 66 nM, with the highest avidity for clones recognizing p34 and p55. The other clones, like those against p14, were considered to display moderate avidity. Of note, all clones with the same peptide specificity used different TCRβ V-segments, pointing at their independent origin and the availability of a broad repertoire (Fig. S2 F). These results demonstrated that the broad repertoire of TEIPP-specific T cells in healthy individuals exhibits a usual functional avidity for their cognate peptide and is competent to respond upon antigen encounter.

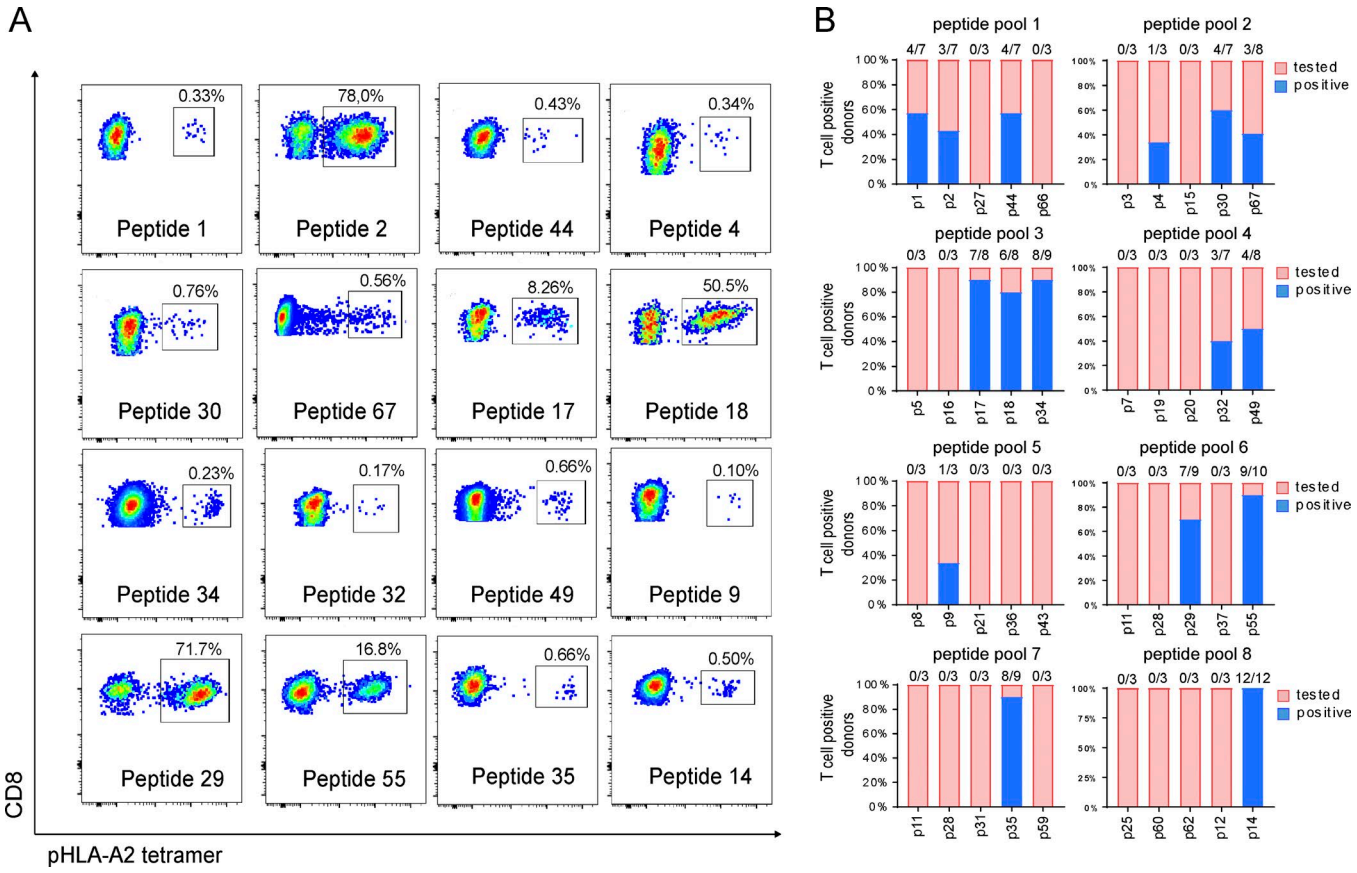

Figure 2. **Detection of CD8⁺ T cells against TEIPP neoantigens in PBMCs of healthy donors.** PBMCs of healthy donors were screened with HLA-A*02:01 tetramers to identify whether a T cell repertoire is present for TEIPP neoantigens. HLA-A*02:01 tetramers folded with the selected 40 TEIPP neoantigen candidates were arranged in eight pools based on predicted peptide binding. **(A)** TEIPP-enriched T cell pools were analyzed by flow cytometry ($n = 3$). Representative dot plots of TEIPP neoantigen-specific CD8⁺ T cells are shown. **(B)** PBMCs of additional healthy donors were tested to validate the presence of a TEIPP T cell repertoire. All 40 TEIPP neoantigen candidates were tested in at least three different donors. Shown are data of all tested donors. Each bar represents one TEIPP neoantigen candidate. Blue indicates the percentage of T cell–positive donors based on flow cytometry analysis. Numbers above each bar indicate the fraction of positive donors out of total tested.

CD8⁺ T cells against p14 recognize TAP-deficient tumors across diverse histological origin

In search for TEIPP antigens on immune-escaped cancers, we selected the p14 peptide-epitope with sequence FLGPWPAAS from the ubiquitously expressed LRPAP1 protein (from now on called $LRPAP1_{21\text{-}30}$) for in-depth examination (Table 1). First, we confirmed specificity for the $LRPAP1_{21\text{-}30}$ epitope for T cell clone 1A8 by testing different peptide length variants of the LRPAP1 signal peptide (Fig. S3 A). Although unconventional, this examination confirmed the serine amino acid as C-terminus for this HLA-A*02:01 allele. Next, LRPAP1 gene expression data were collected from the Cancer Genome Atlas database for different tumor types, revealing that its expression is ubiquitous with exceptionally high expression levels in skin melanomas (Fig. 4 A). We therefore selected the HLA-A*02:01–positive skin melanoma cell line 518A2 and confirmed the expression of the LRPAP1 gene (Fig. 4 A and Fig. S3 B). For this cell line, a TAP1 KO variant, a CRISPR/CAS9 control TAP1-WT variant, and a TAP1/antigen double KO variant were generated by CRISPR/CAS9 technology; these gene-edited variants were tested for recognition by the $LRPAP1_{21\text{-}30}$-specific CD8⁺ T cell clone 1A8 (Fig. 4 B and Fig. S3, C and D). Surface display of HLA-A*02:01 decreased after knocking out the gene for the peptide transporter TAP1 (Fig. 4 C). The $LRPAP1_{21\text{-}30}$-specific CD8⁺ T cell clone selectively recognized the TAP1-deficient variant of 518A2. This suggested that the $LRPAP1_{21\text{-}30}$ signal peptide was only presented by the TAP-deficient tumor variant, despite equal expression of the *LRPAP1* gene and lower HLA-A*02:01 levels on these cells (Fig. 4 D). Furthermore, selective KO of the epitope ($LRPAP1_{21\text{-}30}$ Ag-KO) resulted in complete abrogation of T cell recognition (Fig. 4 D). To control for artificial CRISPR/CAS9-induced immunogenicity, we included a previously established T cell clone (HSS1 PRAME) that recognizes the TAP-dependent PRAME (SLL QHLIGL) tumor antigen. This $PRAME_{425\text{-}433}$-specific CD8⁺ T cell only recognized 518A2 WT cells, whereas it completely failed to respond toward the TAP KO variant. In contrast, $LRPAP1_{21\text{-}30}$-specific T cells displayed a clear preference for the TAP KO variant (Fig. 4 E). Collectively, these data confirmed that the applied tetramer-based selection approach allows the isolation of functional CD8⁺ T cells with a bona fide specificity for the antigen from which the TEIPP was derived. Moreover, these data excluded potential cross-reactivity of T cell clone 1A8 against other peptides presented by the 518A2 melanoma cells. Finally, antibodies against HLA-I molecules were able to block the tumor recognition by T cells, demonstrating dependency on peptide/HLA-I (Fig. 4 F).

Table 1. **Overview of TEIPP neoantigen candidates**

#	Gene name	Peptide sequence[a]	Accession number[b]	HLA-A2 affinity (IC50)[c]	Expression[d]			T cell repertoire
					Tissue[e]	Normal	Cancer	
Ubiquitous TEIPP								
p1	*ERGIC3*	FLSELQYYL	Q9Y282	2	All	++	++	4/7
p4	*TTYH3*	ALFSFVTAL	Q9C0H2	10	All	+	+	1/3
p9	*IGJ*	VLAVFIKAV	P01591	52	All	++	++	1/3
p14	*LRPAP1*	FLGPWPAAS	D6REW6	353	All	++	++	14/14
p29	*ARSA*	LLALAAGLAV	P15289	79	All	++	++	9/10
p44	*EMILIN2*	FLYPFLSHL	Q9BXX0	4	All	+	++	4/7
p49	*H2AFV*	ILEYLTAEV	E5RJU1	30	All	++	++	6/9
p67	*SEP15*	LSEKLERI	O60613	15	All	+	+	4/8
Tissue-specific TEIPP								
p2	*IL12A*	VLLDHLSLA	P29459	7	Mixed	+	+	3/7
p17	*HPR*	LLWGRQLFA	P00739	24	Liver	+++	+	6/7
p18	*FSTL4*	TLLGASLPA	Q6MZW2	27	Mixed	+	+++	5/7
p30	*IFI30*	LLLDVPTAAV	M0QZG3	10	Mixed	++	++	5/8
p32	*CD79B*	LLLSAEPVPA	P40259	41	Lymphoid	+	++	3/7
p34	*PCDHGA6*	LTLLGTLWGA	Q9Y5G7	24	Mixed	+/−	+/−	8/8
p35	*C20orf141*	SVLWLGALGL	Q9NUB4	161	Testis	+	+	16/16
p55	*APCS*	VIIKPLVWV	P02743	113	Liver	+++	+++	9/10

[a]Peptide sequences of the non-mutated neoantigens.
[b]UniProt accession numbers.
[c]Predicted peptide affinity binding in HLA-A2:01.
[d]Protein expression scores are based on data from the Human Protein Atlas.
[e]Protein expression based on the Cancer Genome Atlas database score.

The ubiquitous expression of the *LRPAP1* gene in diverse tumor types prompted us to test T cell recognition of other HLA-A*02:01–positive melanomas and tumors of other histological origin, including renal cell carcinoma and lymphoma. The panel of T1 and T2 lymphoma cells is known for its characterized genomic TAP status (Fig. S3 E; Wei and Cresswell, 1992; Anderson et al., 1993). We confirmed equal *LRPAP1* gene expression by quantitative PCR (qPCR; Fig. S3 F) and examined recognition by multiple $LRPAP1_{21\text{-}30}$-specific T cell clones (Fig. 4 G). All tested $CD8^+$ T cell clones selectively recognized the TAP-deficient T2 cells, again displaying a typical TEIPP specificity.

Next, a panel of HLA-A*02:01–positive TAP-deficient melanomas and renal cell carcinomas was generated by genetically disrupting the *TAP1* gene. Tumor cell mRNA levels of the *LRPAP1* gene were again comparable as quantified by PCR (Fig. S3 G). Flow cytometry analysis revealed that HLA-A*02:01 levels varied between the lines, but that these decreased after *TAP1* gene KO (Fig. 4 H). As observed for the 518A2 melanoma and the T2 lymphoma, multiple $LRPAP1_{21\text{-}30}$-specific T cell clones exhibited a preferential recognition of the TAP1-deficient tumor lines (Fig. 4 I). Interestingly, some parental tumors were already recognized even before silencing the *TAP1* gene (e.g., melanoma 93.04), implying that low endogenous *TAP1* levels in some primary tumors already allow presentation of the $LRPAP1_{21\text{-}30}$ antigen. Indeed, qPCR confirmed low *TAP1* gene expression in the melanoma 93.04 (Fig. S3 H). In line with this, complete abolishment of the *TAP1* gene in tumor line 93.04 did not result in much improved T cell recognition (Fig. 4 I). To further corroborate the shared character across multiple tumor types, we also tested T cell recognition of our 1A8 clone against two colon carcinomas (Fig. S3, I and J). Interestingly, we observed specific T cell responses toward the TAP KO variants of these two colon carcinoma cell lines (Fig. S3 K). Overall, these data clearly demonstrated that the $LRPAP1_{21\text{-}30}$ TEIPP epitope is universally presented in HLA-A*02:01 by cancers of diverse histology when the peptide transporter TAP is not functional. TEIPP-specific $CD8^+$ T cells enable targeting of this shared, non-mutated peptide on immune-escaped $HLA\text{-}I^{low}$ cancers.

Targeting TEIPP antigens appears safe despite ubiquitous expression of their proteins in healthy cells

The fact that human TEIPP antigens derive from ubiquitously expressed non-mutated proteins may raise concerns for autoimmune pathology. Indeed, the LRPAP1 protein is clearly expressed in several critical organs of our body, as revealed by tissue slide staining images available from the Human Protein Atlas (Fig. 5 A and Fig. S4 A; Uhlén et al., 2015). Therefore, two primary melanocyte cultures and two immortalized kidney cell

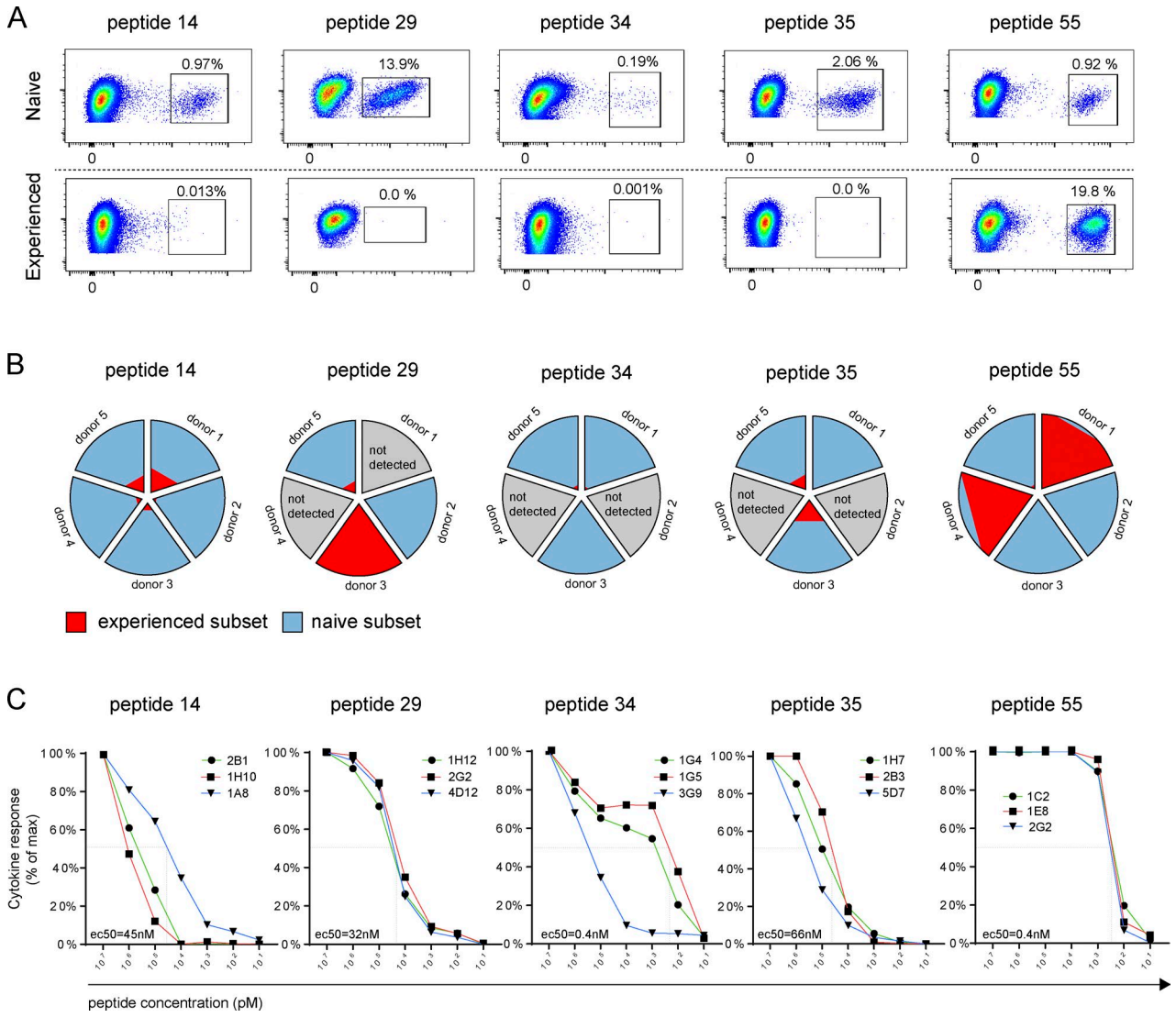

Figure 3. **Most TEIPP-specific CD8⁺ T cells reside in the naive repertoire.** The status and functional avidity of TEIPP-specific T cell peptide candidates p14, p29, p34, p35, and p55 were examined. CD8⁺ T cells to these peptides were most abundantly detected in PBMCs of healthy donors. **(A)** Representative dot plots of pHLA-A*02:01 tetramer–stained CD8⁺ T cells cultured from either the naive subset or the experienced subset. Percentages represent pHLA-A*02:01 tetramer–positive cells out of total CD8⁺ T cells. **(B)** Pie charts for each of the TEIPP neoantigen candidates. Five donors were tested, and each slice represents one donor. The relative percentage of naive cells (blue) and percentage of experienced cells (red) are calculated out of total pHLA-A*02:01 tetramer–positive CD8⁺ cells. **(C)** T cell clones against these peptides were generated by single-cell sorting on HLA-A*02:01 tetramer–positive cells and subsequent expansion. Functional T cell avidity was examined by measuring cytokine production of activated T cells recognizing TEIPP peptide–pulsed, HLA-A*02:01–positive T2 cells with different concentrations of peptide. EC50 was determined by calculating the peptide concentration (nanomolar) corresponding to the 50% cytokine production of the maximum response. Individual clones were tested at least three times.

lines were tested for CD8⁺ T cell recognition. These nontransformed cells contained similar high levels of LRPAP1 transcripts as the 518A2 tumor (Fig. 5 B) and displayed sufficient levels of HLA-A*02:01 at their cell surface (Fig. 5 C). Despite these optimal conditions, $LRPAP1_{21-30}$-specific T cells did not respond to these healthy cells (Fig. 5 D). Exogenous loading of synthetic LRPAP1 peptide to the cells, however, did lead to LRPAP1-specific T cell response, suggesting that healthy cells were capable of presenting peptides (Fig. 5 E). These data confirmed a crucial role for low TAP function for the presentation of TEIPP antigens and suggested that TEIPP targeting might be considered a safe therapy, even though these proteins are present in healthy tissues as well.

In summary, our data reveal an array of novel non-mutated tumor antigens displayed by tumors with (partial) TAP deficiency (Table 1). Some of these are tissue restricted, but others, like the LRPAP1 signal peptide, are ubiquitously expressed and represent universal HLA-presented tumor antigens on cancers with impaired antigen processing.

Discussion

We developed a screening approach to identify human antigens belonging to the novel category of non-mutated neoantigens of self origin called TEIPP. Our screen yielded 65 potential TEI PP candidates, which are exclusively present in the peptidome

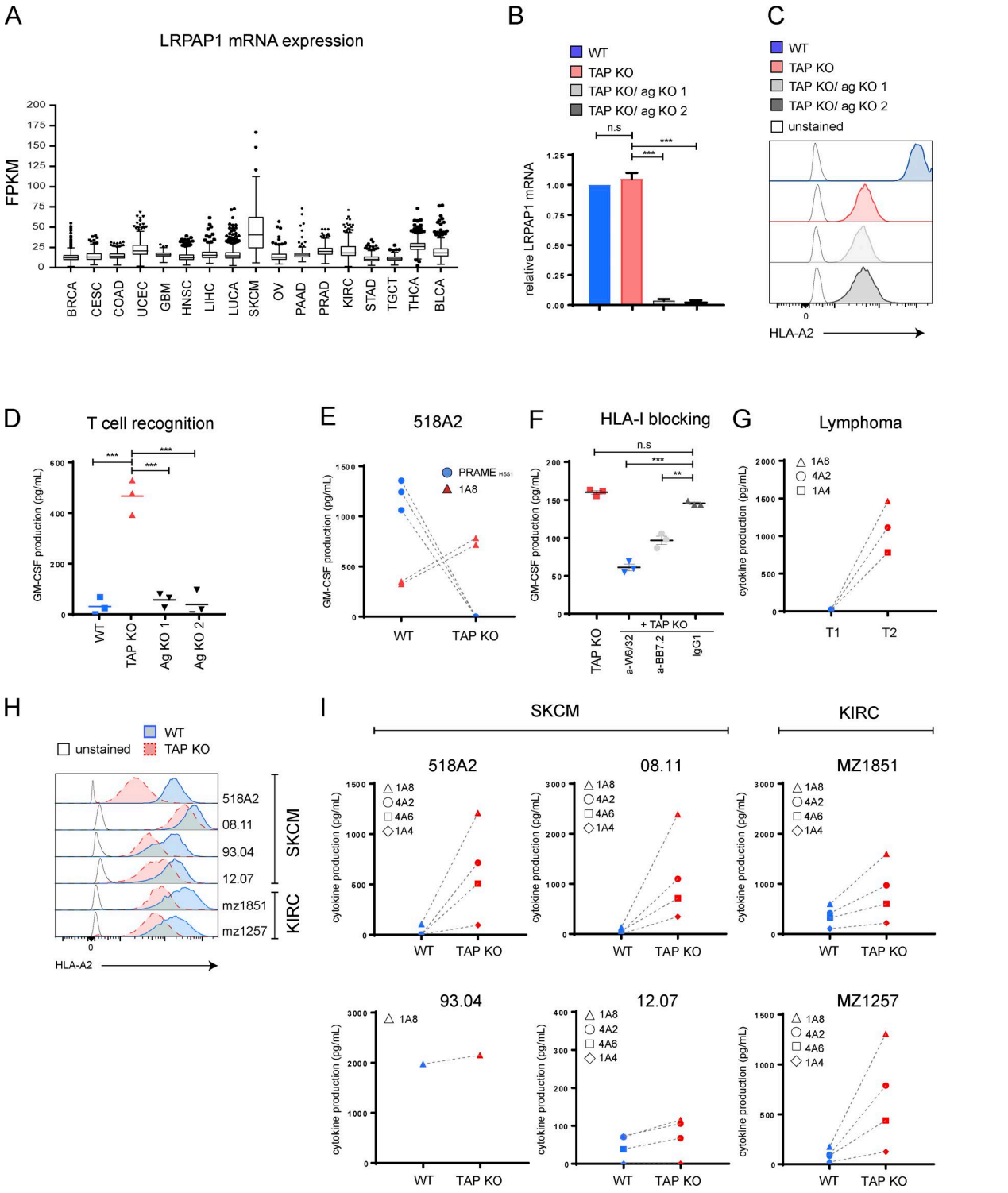

Figure 4. **CD8⁺ T cells against p14 recognize TAP-deficient tumors of different histological origin.** T cell clones were tested for their specificity to selectively recognize the LRPAP1$_{21\text{-}30}$ TEIPP epitope presented on TAP-impaired tumors. **(A)** Whisker plots of LRPAP1 gene expression in human cancers collected from the Cancer Genome Atlas database. **(B)** The TAP1 gene in the melanoma 518A2 was knocked out (TAP KO) using CRISPR/CAS9. In addition, the LRPAP1$_{21\text{-}30}$ epitope was knocked out in these cells (ag KO). mRNA expression of LRPAP1 was examined by qPCR. Data are shown as mean ± SD of triplicates. Significance testing: unpaired Student's *t* test; n.s., not significant; ***, P < 0.001 (*n* = 3). **(C)** HLA-A*02:01 surface expression on 518A2 melanoma variants measured by flow cytometry. Plots are representative of three independent experiments. **(D)** GM-CSF production of T cell clone 1A8 upon 518A2 TAP KO recognition. When LRPAP1$_{21\text{-}30}$ epitope was knocked out (ag KO), recognition by the T cells was abolished. Representative data of three independent experiments are shown. Each dot represents a technical replicate. Significance testing: Student's unpaired *t* test; ***, P < 0.001. **(E)** To control for artificial CRISPR/CAS9-mediated immunogenicity, we cocultured T cell clones specific for LRPAP1$_{21\text{-}30}$ (TAP-independent epitope) or PRAME$_{425\text{-}433}$ (TAP-dependent epitope) together with the 518A2 melanoma (WT versus TAP KO). GM-CSF cytokine response was measured. Each dot represents one independent experiment with technical triplicates. **(F)** HLA dependency was tested using HLA-ABC– or HLA-A*02:01–blocking antibodies. Representative data of two independent experiments are shown. Each

of cancer cells. Analysis of the 40 HLA-A*02:01–binding TEIPP candidates revealed a consistent $CD8^+$ T cell repertoire to 16 of these 40 peptides. Additional analyses demonstrated that these $CD8^+$ T cells were present in the naive pool for five peptide candidates and that they were not affected by central or peripheral tolerance. Monoclonal T cell cultures against the TEIPP epitope $LRPAP1_{21\text{-}30}$ selectively recognized TAP1-deficient cancers from different histological origins, including lymphoma, melanoma, colon carcinoma, and renal cell carcinoma, whereas TAP-proficient primary cells were spared from T cell recognition. This emphasizes the attractiveness of targeting TEIPP neoantigens on HLA-I^{low} cancers, namely for its shared character on those tumor cells. Thus far, we focused on HLA-A*02:01–binding TEIPP peptides, but our screen also predicted a broad array of antigens presented by other HLA types. Furthermore, we realize that this proof-of-concept approach is far from complete. Most likely, many more undiscovered pathways enable the presentation of TAP-independent processed TEIPP neoantigens.

We observed that knocking out the *TAP1* gene rendered all tested cancer cell lines vulnerable for TEIPP-specific T cells. Importantly, TEIPP-specific T cells exhibited moderate to high recognition of some WT skin melanomas and renal cell carcinomas (e.g., 93.04, mz1257), and CRISPR/CAS9-mediated KO of the *TAP1* gene led to only modest improvement of cancer cell recognition. In other cancer lines (e.g., melanoma 518A2, 08.11), minimal T cell responses were detected to WT cancer cells, and knockdown of TAP1 was necessary to induce strong T cell recognition. These data suggested that some cancer cell lines already down-modulated TAP1 gene expression to such a degree that it was already sufficient for the presentation of TEIPP neoantigens. Although only 1–2% of melanomas have deleterious mutations in TAP1 or TAP2, a high frequency of metastatic melanomas displays low TAP1 expression due to epigenetic silencing (Garrido et al., 2016; Ritter et al., 2017). At this moment, we have not determined how low TAP1 function needs to be for TEIPP neoantigens to be presented on the cell surface of cancer cells. The exact mechanisms of selective TEIPP neoantigen presentation on antigen-processing defective cells are still not completely known. Our previous experiments in mouse models suggested a competition between peptide antigens in the ER (Oliveira et al., 2011; Viganò et al., 2012). The peptide-loading complex (PLC) is a multisubunit membrane complex orchestrating the loading and editing of peptides in HLA-I molecules, facilitated by the TAP1/TAP2 channel, and thereby responsible for the translocation of peptides from the cytosol into the PLC (Blees et al., 2017). The TAP peptide transporter is incorporated in this efficient PLC, in close proximity to HLA-I molecules, which could explain why peptides processed through different mechanisms, independent of TAP, will not have the chance to bind in HLA-I molecules. Besides TAP levels, the amount of available antigenic protein also needs to be taken into account. Interestingly, massive overexpression of a TEIPP antigen makes it possible to present its TEIPP peptide in the cell surface even in TAP-proficient cells (Oliveira et al., 2011). We theorize that these two factors govern the efficiency of TEIPP neoantigen presentation. Low TAP function allows for low antigen expression, whereas moderate TAP function needs higher amounts of antigen expression (Durgeau et al., 2011; Oliveira et al., 2011). Of utmost importance is that TAP function in healthy cells of our organs is high enough to prevent recognition by TEIPP-specific T cells (Doorduijn et al., 2016, 2018a).

The presence of a TEIPP T cell repertoire in healthy donors indicates that no negative selection has occurred in the thymus, even though gene expression in the thymus was observed for most of the TEIPP neoantigen candidates (Fig. S4 B). During T cell education in the thymus, TEIPP-specific T cells are positively selected for low affinity interaction with peptide/MHC in the cortex of the thymus. To prevent autoimmune responses, negative selection of T cells in the medulla of the thymus is essential to delete self-reactive T cells. This strengthens the hypothesis that TAP-proficient medullary thymic epithelial cells might express the target proteins but do not present TEIPP antigens by their HLA-I, and thus TEIPP T cells will undergo normal thymic selection. Indeed, TEIPP-specific T cells are deleted from the repertoire of TAP-deficient mice (Doorduijn et al., 2016). Moreover, most of the evaluated TEIPP-specific T cells were only found in the naive pool in the circulation and have not encountered antigen yet, signifying that TAP-proficient healthy cells did not trigger TEIPP-specific immunity. Although not tested, we presume this T cell repertoire to be naive in cancer patients as well, since tumor cells are not real APCs and harbor an immune-suppressive environment. Moreover, some viruses that down-modulate TAP (e.g., HSV and CMV) might also manipulate other pathways and therefore not allow TEIPP T cell priming. Ex vivo T cell activation or in vivo vaccination strategies might be needed to recruit the TEIPP T cell repertoire for immunotherapy. These assumptions are based on our earlier observations in a mouse model for TEIPP (Doorduijn et al., 2018a). It is noteworthy that, in some donors, we observed that T cells against p29 and p55 were derived from the antigen-experienced pool. We speculate that these TEIPP specificities had been triggered by cross-reactivity to microbiota-derived epitopes leaked from the gut, which can occur after the use of antibiotics or other intestinal injury (Lee et al., 2011; Zitvogel et al., 2016). Since the tested healthy donors did not suffer from severe autoimmune reactivity, even antigen-experienced TEIPP-specific T cells apparently do not target healthy TAP-proficient tissues. The safety of TEIPP-targeting therapies was thoroughly evaluated in mouse tumor models (van Hall et al., 2006; Chambers et al., 2007; Doorduijn et al., 2016, 2018a,b).

dot represents a technical replicate. Significance testing: unpaired Student's *t* test; n.s., not significant; **, P < 0.01; ***, P < 0.001. **(G)** TEIPP T cell specificity was determined by coculturing three different T cell clones together with TAP-proficient T1 cells and TAP-deficient T2 lymphoma cells. Cytokine responses were measured to detect T cell recognition. Representative data of three independent experiments with technical triplicates are shown. **(H)** HLA-A*02:01 surface expression of the TAP-impaired tumor panels as measured by flow cytometry (SKCM, melanoma; KIRC, renal carcinoma). Representative data of three independent experiments are shown. **(I)** Cytokine production of indicated T cell clones upon antigen recognition of four melanomas and two renal carcinomas. Each dot represents one T cell clone specific for the $LRPAP1_{21\text{-}30}$ epitope. Representative data of three independent experiments with technical triplicates are shown.

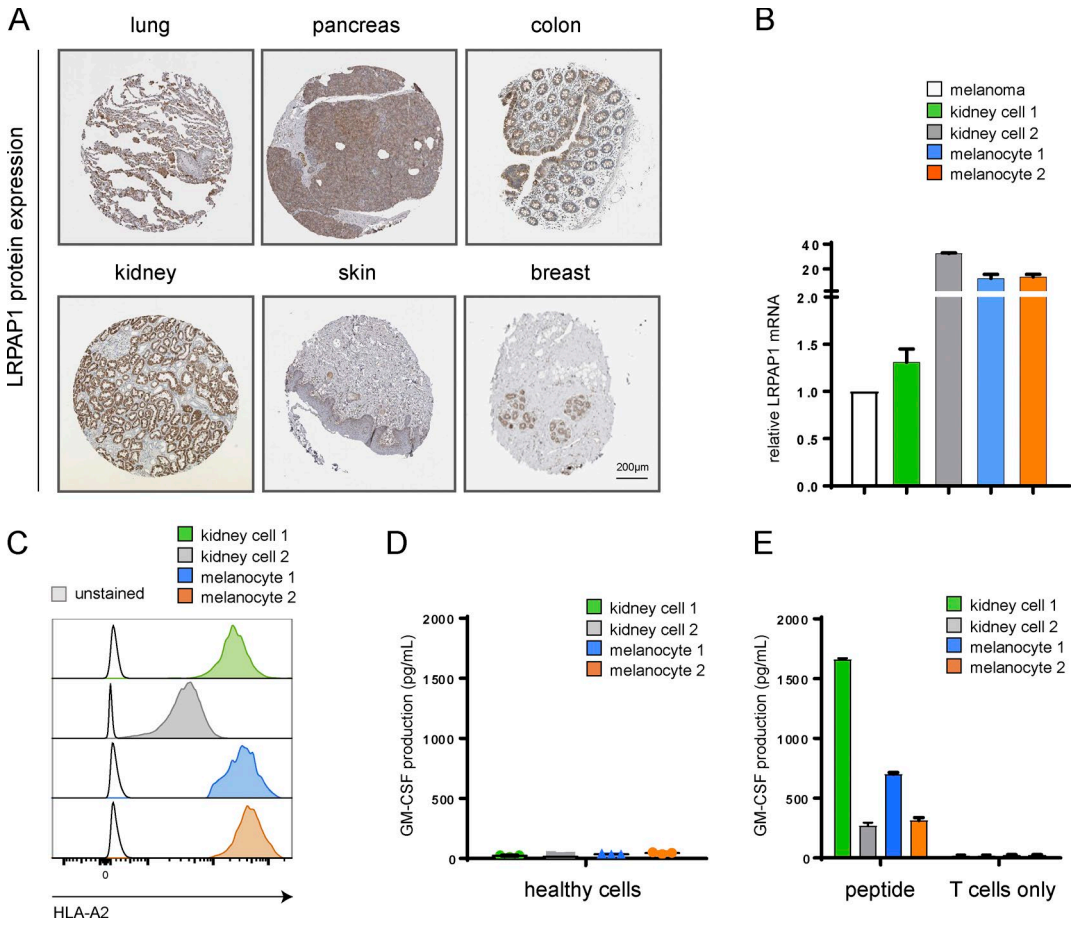

Figure 5. **Targeting TEIPP antigens is safe despite ubiquitous expression of their proteins in healthy cells.** To assess the safety of targeting non-mutated TEIPP neoantigens, we examined the T cell recognition of healthy cells. **(A)** Histological tissue stainings for LRPAP1 were collected from an online-accessible database (the Human Protein Atlas). Positive protein detection was observed in various healthy organs. **(B)** *LRPAP1* mRNA levels were determined of two primary melanocyte cultures and two nontransformed kidney epithelial cell lines by qPCR. Data are shown as mean ± SD from one out of two experiments. **(C)** Surface HLA-A*02:01 expression of the healthy cells was determined by flow cytometry. Representative data of three independent experiments are shown. **(D)** No cytokine responses were detected when T cells specific for $LRPAP1_{21\text{-}30}$ were cocultured with these healthy cells. **(E)** To assess the ability of the healthy cells to present the epitope in HLA-A*02:01, peptide was exogenously loaded. $LRPAP1_{21\text{-}30}$-specific T cell clone 1A8 was cocultured with peptide-pulsed healthy cells, and GM-CSF cytokine production was measured. **(D and E)** Representative triplicate data of two independent experiments are shown.

Vaccine-induced TEIPP-specific T cells via synthetic peptides or dendritic cells, or adoptive transfer of TEIPP-specific T cells, all reduced outgrowth of TAP-deficient tumors without any sign of autoimmune reactivity.

TEIPP neoantigens are selectively presented in cancer cells with deficient function of MHC-I–processing machinery. Therefore, we anticipate a complementary role for these antigens to those of other categories, like patient-specific mutanome peptides or cancer-testis antigens. A combination of these might prevent immune escape via shutdown of HLA-I expression due to defects in the antigen-processing machinery. A great asset of TEIPP antigens is their non-mutated status and the fact that the tumor antigens are broadly shared across many cancer types. A few validated TEIPP antigens or gene transfer of their cognate-cloned T cell receptors might be sufficient for increased efficacy of immunotherapy through prevention of tumor escape. Future investigations need to reveal safety and applicability of vaccination-based strategies and TCR-based gene transfer approaches for TEIPP. Together, we propose that TEIPP neoantigens are an interesting way to reestablish antitumor responses in human immune-escaped cancers.

Materials and methods

Study design

The aim of this study was to test a systematic, hybrid, forward-reversed immunology approach to identify TEIPP-specific T cells and their cognate antigen (Table 1). For this, we collected the whole human proteome dataset from UniProt (ID: 9606, Release: 2014_06). For predictions of the N-terminal signal cleavage location and the topology prediction for C-terminal tail peptides, the web-based topology algorithm Phobius was used. For N-terminal peptide candidates, proteins with a predicted signal peptide probability of >0.5 were included. For C-terminal peptide candidates, proteins with a predicted C-terminal tail located in the ER were included. Peptide binding affinity to HLA-I molecules was predicted using MHCnet4.0 (http://www.cbs.dtu.dk/services/NetMHC/). Peptides with a predicted binding affinity <500 nM

were included. We used the peptidome elution library (release 2014_10) of the Tübingen group (Department of Immunology, University of Tübingen) to select for biologically processed peptides. Next, in vitro analysis was performed on 40 HLA-A*02:01 TEIPP candidates using healthy donor PBMCs. In-depth analysis was performed on five TEIPP candidates. To guarantee statistical power, we performed all experiments on at least three different PBMC batches isolated from different donors.

Tumor cell lines

Human tumor cell lines were obtained through ATCC or derived from patient surgery material. The clinical protocol was approved by the Medical Ethics Committee of the Leiden University Medical Center and conducted in accordance with the Declaration of Helsinki. All tumor cell lines were cultured at 37°C, 5% CO_2, in DMEM (Invitrogen) containing 8% heat-inactivated FCS, 100 U/ml penicillin, and 100 µg/ml streptomycin (Life Technologies) and supplemented with 2 mM glutamine (Invitrogen).

Generation of TEIPP-specific T cell clones

Buffy coats from healthy donors were obtained from Sanquin (Sanquin blood facility). Informed consent was given in writing by all participants. PBMCs were isolated using a ficoll gradient (density 1.077 g/ml). Approximately 500 × 10^6 PBMCs were incubated with PE-pHLA-A*02:01 tetramers for 30 min at 4°C. Anti-PE magnetic beads (MACS) were used to pull out pHLA-A*02:01 tetramer–positive cells over a MACS LS column as instructed by the manufacturer (Miltenyi Biotech). T cells were cultured in complete IMDM containing 8% human serum (Sanquin blood facility) and 100 U/ml IL-2 (Proleukine; Novartis). Bulk T cells were stimulated every 2 wk with a mixture of T cells (10^6), 10 µM synthetic peptide, irradiated PBMCs (10^6 cells, 80 Gy), and EBV-JY (10^5 cells, 100 Gy) in complete T cell culture medium supplemented with 100 U/ml IL-2 in 24-well plates (Costar). Culture medium was replenished every 2–3 d with fresh complete T cell medium. After two rounds of specific stimulation, the polyclonal T cell bulk was incubated with PE-labeled tetramers and single-cell sorted using flow cytometry to obtain monoclonal T cells. After monoclonal cell sorting, T cell clones were stimulated with a PHA mixture in 1 well of a 96-well plate: complete T cell medium supplemented with 800 ng/ml PHA (Murex Biotech), 100 U/ml IL-2, irradiated PBMCs (50 × 10^5 cells, 80 Gy), and EBV-JY cells (10 × 10^4 cells, 100 Gy).

Generation of pHLA-A*02:01 tetramers

Ultra-pure peptides were synthesized by JPT Peptide Technologies. Recombinant HLA-A*02:01 and human β2m proteins were in-house synthesized in *Escherichia coli* (Garboczi et al., 1992; Burrows et al., 2000). Biotinylated HLA-A*02:01 molecules were produced containing a UV-sensitive peptide to enable easy transfer of specific peptide, as previously described (Bakker et al., 2008). In brief, HLA-A*02:01 complexes were purified by gel filtration using fast protein liquid chromatography. pHLA-A*02:01 complexes were exposed to UV light to facilitate peptide exchange, resulting in peptide-specific monomers. pHLA-A*02:01 tetramers were formed by coupling biotinylated pHLA-A*02:01 monomers with streptavidin-coupled R-PE (Thermo Fisher). Tetramers were stored at −80°C for long-term storage or 4°C for short-term storage.

Coculture T cell reactivity assay

Dependent on the T cell clone, GM-CSF (T cell clone 1A8 and PRA ME) or IFN-γ (all other tested T cell clones) ELISA assays (GM-CSF, MabTech; IFN-γ, PeliKine) were used to measure the cytokine production of activated T cells. ELISA plates were coated with human IFN-γ or GM-CSF primary antibody overnight at 4°C. T cell–conditioned medium was collected and incubated in the precoated ELISA plates for 2 h at room temperature. Next, ELISA plates were washed with PBS with 0.1% Tween-20 followed by incubation with the HRP-conjugated secondary antibody for 1 h. ELISA plates were developed with TMB (3,3,5,5-tetramethyl-benzidine liquid substrate supersensitive, for ELISA; Sigma-Aldrich) and measured at 450 nm using a plate reader (Spectramax id3; Molecular Devices). Lower cut-off values for cytokine production were calculated as medium values plus three times the SD. Values below this threshold were considered negative. All plotted values were within the upper and lower detection limits of the ELISAs.

Affinity and stability assay

Peptide affinity and stability were determined as previously described (van der Burg et al., 1996; Harndahl et al., 2012). In brief, HLA-A*02:01$^+$ T2 cells were pulsed with increasing concentrations of peptide (1–100 µM) in serum-free RPMI culture medium for 24 h at 37°C. For MHC:peptide affinity, the maximum HLA-A*02:01 expression was measured by flow cytometry to calculate the EC50 concentration. For MHC:peptide stability, HLA-A*02:01–positive T2 cells were pulsed with 100 µM peptide for 24 h at 37°C. Maximum HLA-A*02:01 expression was determined and followed over time to calculate the $t_{1/2}$ value.

Generation of gene KOs in tumor cells using CRISPR/CAS9

Single guide RNAs (sgRNAs) were designed to target exon 1 of the human TAP1 gene (sgTAP1: 5′-GCTGCTACTTCTCGCCGACT-3′) or the $LRPAP1_{21\text{-}30}$ epitope located in exon 1 ($LRPAP1_{21\text{-}30}$: 5′-AGGGTCAGGTCGTTTCTGCG-3′). The sgRNA target sequence was cloned into the lentiCRISPR v2 vector (Sanjana et al., 2014). Virus particles were generated by cotransfecting sgRNA/CAS9 containing plasmid together with PAX2/pMD2.G packaging vectors into HEK293T cells using Lipofectamine 2000 (Thermo Fisher). Tumor cells were incubated with medium containing the virus particles for 24 h, and transduced tumor cells were selected with 1–5 µg/ml puromycin (Gibco). TAP1 KO efficiency was analyzed by measuring surface HLA-ABC (w6/32; BioLegend) expression using flow cytometry. Polyclonal TAP KO cell lines were generated by FACS sorting the HLA-I^{low} cell population. CRISPR/CAS9 TAP-WT control cells were generated by FACS sorting the HLA-I^{high} cell population of the polyclonal bulk. TAP1 expression was verified by Western blot using anti-TAP1 antibodies (Cell Signaling).

Western blot

Proteins from cell cultures were extracted in lysis buffer (radioimmunoprecipitation assay; Cell Signaling), and protein concentrations were assessed using the Bradford Protein Assay

Kit (Thermo Fisher). Protein samples were separated on a 4–12% SDS-PAGE gel and transferred onto nitrocellulose membranes using semi-dry transfer (Bio-Rad). To prevent nonspecific binding, membranes were blocked with 5% milk in Tris-buffered saline with 0.1% Tween-20 for 1 h at room temperature. The following antibodies were used: anti-TAP1 (dilution 1:1,000, 4°C; Cell Signaling), anti–β-actin (dilution 1:1,000, 4°C; Cell Signaling), and HRP-linked mouse anti-rabbit IgG (dilution 1:5,000, room temperature; Cell Signaling).

Flow cytometry analysis

CD3 (SK7), CD4 (SK3), CD8 (SK1), CD45RO (UCHL1), HLA-A*02:01 (bb7.2; BD Biosciences), and HLA-ABC (MCA81A), CD45RA (HI100), CD62L (DREG-56; BioLegend) anti-human mAbs were used for flow cytometry analysis. Cells were incubated with mAbs for 30 min at 4°C and washed three times. Unstained cells were used as negative controls. The Vβ repertoire analysis kit was used to determine the TCR Vβ of the different monoclonal T cells (Beckman Coulter). For T cell specificity analysis, we incubated T cells with pHLA-A*02:01 tetramers for 30 min at room temperature and washed three times. T cells were considered tetramer positive when mean fluorescence intensity was at least 10^2 times higher than unstained control. Cells were measured using an LSR-II flow cytometer (BD Biosciences) and analyzed using FlowJo software version 10 (Tree Star).

mRNA isolation, cDNA synthesis, and qPCR analysis

Cell pellets were washed twice with PBS and snap-frozen in liquid nitrogen. RNA was isolated using the RNAeasy Kit (Qiagen) according to the manufacturer's protocol. cDNA was synthesized using the High Capacity RNA-to-cDNA Kit (Applied Biosystems). qPCR was done using SYBR Green supermix (Bio-Rad). For qPCR analysis, we used the following primers: GAPDH_f: 5′-GTGCTGAGTATG TCGTGGAGTCTAC-3′; GAPDH_r: 5′-GGCGGAGATGATGACCCT TTTGG-3′; TAP1_f: 5′-CTTGCAGGGAGAGGTGTTTG-3′; TAP1_r: 5′-GAGCATGATCCCCAAGAGAC-3′; LRPAP1_f: 5′-GACCGAAGA AATCCACGAGA-3′; LRPAP1_r: 5′-AGGTCCCACAGGTCAATCAC-3′.

Statistical analysis

All data are presented as means and SD. Statistical analysis was done using a paired Student's *t* test (two-tailed) to determine the statistical significance of the differences. A minimum of three technical replicates were used in all experiments and were repeated at least two times.

Online supplemental material

Table S1 shows an overview of the number of histological tissue samples and cancer samples that are used to create the peptide elution database. In Fig. S1, we plotted the results of the predicted TEIPP candidate peptide binding in HLA-I. Fig. S2 shows the characterization of TEIPP T cells, sequence, binding affinity and stability of the TEIPP antigens, and homology with bacterial peptides. In Fig. S3, mRNA and protein expression analysis of LRP AP1 and TAP1 on the tumor panel and functional T cell assays are shown to support the findings in Fig. 4 in the main text. Fig. S4 illustrates the protein expression analysis of TEIPP candidates in healthy and cancer tissue.

Acknowledgments

We thank the peptide synthesis core facility and the flow cytometry core facility of the Leiden University Medical Center for their contribution to this project. The peptide elution database was made available by the Department of Immunology, University of Tübingen.

This work was supported by the Dutch Cancer Foundation (2013-6142 to K.A. Marijt).

The authors declare no competing financial interests.

Author contributions: T. van Hall and S.H. van der Burg designed the project. K.A. Marijt and L. Blijleven performed and designed all experiments. M.G. Kester and K.A. Marijt synthesized the tetramers. E.M.E. Verdegaal provided all cancer cell lines. K.A. Marijt and T. van Hall wrote the manuscript. D.J. Kowalewski performed peptide matching analysis. H.-G. Rammensee and S. Stevanović shared their peptidome databases. K.A. Marijt, T. van Hall, and S.H. van der Burg interpreted data. S.H. van der Burg, H.-G. Rammensee, S. Stevanović, and M.H.M. Heemskerk reviewed and edited the manuscript.

Submitted: 23 March 2018
Revised: 30 May 2018
Accepted: 10 July 2018

References

Anderson, K.S., J. Alexander, M. Wei, and P. Cresswell. 1993. Intracellular transport of class I MHC molecules in antigen processing mutant cell lines. *J. Immunol.* 151:3407–3419.

Andreatta, M., and M. Nielsen. 2016. Gapped sequence alignment using artificial neural networks: application to the MHC class I system. *Bioinformatics.* 32:511–517. https://doi.org/10.1093/bioinformatics/btv639

Bakker, A.H., R. Hoppes, C. Linnemann, M. Toebes, B. Rodenko, C.R. Berkers, S.R. Hadrup, W.J. van Esch, M.H. Heemskerk, H. Ovaa, and T.N. Schumacher. 2008. Conditional MHC class I ligands and peptide exchange technology for the human MHC gene products HLA-A1, -A3, -A11, and -B7. *Proc. Natl. Acad. Sci. USA.* 105:3825–3830. https://doi.org/10.1073/pnas.0709717105

Blees, A., D. Januliene, T. Hofmann, N. Koller, C. Schmidt, S. Trowitzsch, A. Moeller, and R. Tampé. 2017. Structure of the human MHC-I peptide-loading complex. *Nature.* 551:525–528.

Blum, J.S., P.A. Wearsch, and P. Cresswell. 2013. Pathways of antigen processing. *Annu. Rev. Immunol.* 31:443–473. https://doi.org/10.1146/annurev-immunol-032712-095910

Burrows, S.R., N. Kienzle, A. Winterhalter, M. Bharadwaj, J.D. Altman, and A. Brooks. 2000. Peptide-MHC class I tetrameric complexes display exquisite ligand specificity. *J. Immunol.* 165:6229–6234. https://doi.org/10.4049/jimmunol.165.11.6229

Chambers, B., P. Grufman, V. Fredriksson, K. Andersson, M. Roseboom, S. Laban, M. Camps, E.Z. Wolpert, E.J. Wiertz, R. Offringa, et al. 2007. Induction of protective CTL immunity against peptide transporter TAP-deficient tumors through dendritic cell vaccination. *Cancer Res.* 67:8450–8455. https://doi.org/10.1158/0008-5472.CAN-07-1092

Doorduijn, E.M., M. Sluijter, B.J. Querido, C.C. Oliveira, A. Achour, F. Ossendorp, S.H. van der Burg, and T. van Hall. 2016. TAP-independent self-peptides enhance T cell recognition of immune-escaped tumors. *J. Clin. Invest.* 126:784–794. https://doi.org/10.1172/JCI83671

Doorduijn, E.M., M. Sluijter, K.A. Marijt, B.J. Querido, S.H. van der Burg, and T. van Hall. 2018a. T cells specific for a TAP-independent self-peptide remain naïve in tumor-bearing mice and are fully exploitable for therapy. *OncoImmunology.* 7:e1382793. https://doi.org/10.1080/2162402X.2017.1382793

Doorduijn, E.M., M. Sluijter, B.J. Querido, U.J.E. Seidel, C.C. Oliveira, S.H. van der Burg, and T. van Hall. 2018b. T Cells Engaging the Conserved MHC Class Ib Molecule Qa-1^b with TAP-Independent Peptides Are Semi-Invariant Lymphocytes. *Front. Immunol.* 9:60. https://doi.org/10.3389/fimmu.2018.00060

Durgeau, A., F. El Hage, I. Vergnon, P. Validire, V. de Montpréville, B. Besse, J.C. Soria, T. van Hall, and F. Mami-Chouaib. 2011. Different expression levels of the TAP peptide transporter lead to recognition of different antigenic peptides by tumor-specific CTL. *J. Immunol.* 187:5532–5539. https://doi.org/10.4049/jimmunol.1102060

Dutoit, V., V. Rubio-Godoy, P.Y. Dietrich, A.L. Quiqueres, V. Schnuriger, D. Rimoldi, D. Liénard, D. Speiser, P. Guillaume, P. Batard, et al. 2001. Heterogeneous T-cell response to MAGE-A10(254-262): high avidity-specific cytolytic T lymphocytes show superior antitumor activity. *Cancer Res.* 61:5850–5856.

El Hage, F., V. Stroobant, I. Vergnon, J.F. Baurain, H. Echchakir, V. Lazar, S. Chouaib, P.G. Coulie, and F. Mami-Chouaib. 2008. Preprocalcitonin signal peptide generates a cytotoxic T lymphocyte-defined tumor epitope processed by a proteasome-independent pathway. *Proc. Natl. Acad. Sci. USA.* 105:10119–10124. https://doi.org/10.1073/pnas.0802753105

Gao, J., L.Z. Shi, H. Zhao, J. Chen, L. Xiong, Q. He, T. Chen, J. Roszik, C. Bernatchez, S.E. Woodman, et al. 2016. Loss of IFN-γ Pathway Genes in Tumor Cells as a Mechanism of Resistance to Anti-CTLA-4 Therapy. *Cell.* 167:397–404.e9. https://doi.org/10.1016/j.cell.2016.08.069

Garboczi, D.N., D.T. Hung, and D.C. Wiley. 1992. HLA-A2-peptide complexes: refolding and crystallization of molecules expressed in Escherichia coli and complexed with single antigenic peptides. *Proc. Natl. Acad. Sci. USA.* 89:3429–3433. https://doi.org/10.1073/pnas.89.8.3429

Garrido, F., N. Aptsiauri, E.M. Doorduijn, A.M. Garcia Lora, and T. van Hall. 2016. The urgent need to recover MHC class I in cancers for effective immunotherapy. *Curr. Opin. Immunol.* 39:44–51. https://doi.org/10.1016/j.coi.2015.12.007

Harndahl, M., M. Rasmussen, G. Roder, I. Dalgaard Pedersen, M. Sørensen, M. Nielsen, and S. Buus. 2012. Peptide-MHC class I stability is a better predictor than peptide affinity of CTL immunogenicity. *Eur. J. Immunol.* 42:1405–1416. https://doi.org/10.1002/eji.201141774

Käll, L., A. Krogh, and E.L. Sonnhammer. 2004. A combined transmembrane topology and signal peptide prediction method. *J. Mol. Biol.* 338:1027–1036. https://doi.org/10.1016/j.jmb.2004.03.016

Lauss, M., M. Donia, K. Harbst, R. Andersen, S. Mitra, F. Rosengren, M. Salim, J. Vallon-Christersson, T. Törngren, A. Kvist, et al. 2017. Mutational and putative neoantigen load predict clinical benefit of adoptive T cell therapy in melanoma. *Nat. Commun.* 8:1738. https://doi.org/10.1038/s41467-017-01460-0

Lee, Y.K., J.S. Menezes, Y. Umesaki, and S.K. Mazmanian. 2011. Proinflammatory T-cell responses to gut microbiota promote experimental autoimmune encephalomyelitis. *Proc. Natl. Acad. Sci. USA.* 108(Suppl 1):4615–4622. https://doi.org/10.1073/pnas.1000082107

Leonhardt, R.M., D. Fiegl, E. Rufer, A. Karger, B. Bettin, and M.R. Knittler. 2010. Post-endoplasmic reticulum rescue of unstable MHC class I requires proprotein convertase PC7. *J. Immunol.* 184:2985–2998. https://doi.org/10.4049/jimmunol.0900308

Leonhardt, R.M., N. Vigneron, C. Rahner, and P. Cresswell. 2011. Proprotein convertases process Pmel17 during secretion. *J. Biol. Chem.* 286:9321–9337. https://doi.org/10.1074/jbc.M110.168088

Marijt, K.A., E.M. Doorduijn, and T. van Hall. 2018. TEIPP antigens for T-cell based immunotherapy of immune-edited HLA class I^{low} cancers. *Mol. Immunol.*. https://doi.org/10.1016/j.molimm.2018.03.029

Martoglio, B., and B. Dobberstein. 1998. Signal sequences: more than just greasy peptides. *Trends Cell Biol.* 8:410–415. https://doi.org/10.1016/S0962-8924(98)01360-9

McKee, M.D., J.J. Roszkowski, and M.I. Nishimura. 2005. T cell avidity and tumor recognition: implications and therapeutic strategies. *J. Transl. Med.* 3:35. https://doi.org/10.1186/1479-5876-3-35

Medina, F., M. Ramos, S. Iborra, P. de León, M. Rodríguez-Castro, and M. Del Val. 2009. Furin-processed antigens targeted to the secretory route elicit functional TAP1-/-CD8+ T lymphocytes in vivo. *J. Immunol.* 183:4639–4647. https://doi.org/10.4049/jimmunol.0901356

Müllbacher, A., M. Lobigs, J.W. Yewdell, J.R. Bennink, R. Tha Hla, and R.V. Blanden. 1999. High peptide affinity for MHC class I does not correlate with immunodominance. *Scand. J. Immunol.* 50:420–426. https://doi.org/10.1046/j.1365-3083.1999.00619.x

Neefjes, J., M.L. Jongsma, P. Paul, and O. Bakke. 2011. Towards a systems understanding of MHC class I and MHC class II antigen presentation. *Nat. Rev. Immunol.* 11:823–836. https://doi.org/10.1038/nri3084

Nielsen, M., C. Lundegaard, P. Worning, S.L. Lauemøller, K. Lamberth, S. Buus, S. Brunak, and O. Lund. 2003. Reliable prediction of T-cell epitopes using neural networks with novel sequence representations. *Protein Sci.* 12:1007–1017. https://doi.org/10.1110/ps.0239403

Oliveira, C.C., B. Querido, M. Sluijter, J. Derbinski, S.H. van der Burg, and T. van Hall. 2011. Peptide transporter TAP mediates between competing antigen sources generating distinct surface MHC class I peptide repertoires. *Eur. J. Immunol.* 41:3114–3124. https://doi.org/10.1002/eji.201141836

Oliveira, C.C., B. Querido, M. Sluijter, A.F. de Groot, R. van der Zee, M.J. Rabelink, R.C. Hoeben, F. Ossendorp, S.H. van der Burg, and T. van Hall. 2013. New role of signal peptide peptidase to liberate C-terminal peptides for MHC class I presentation. *J. Immunol.* 191:4020–4028. https://doi.org/10.4049/jimmunol.1301496

Patel, S.J., N.E. Sanjana, R.J. Kishton, A. Eidizadeh, S.K. Vodnala, M. Cam, J.J. Gartner, L. Jia, S.M. Steinberg, T.N. Yamamoto, et al. 2017. Identification of essential genes for cancer immunotherapy. *Nature.* 548:537–542. https://doi.org/10.1038/nature23477

Ritter, C., K. Fan, A. Paschen, S. Reker Hardrup, S. Ferrone, P. Nghiem, S. Ugurel, D. Schrama, and J.C. Becker. 2017. Epigenetic priming restores the HLA class-I antigen processing machinery expression in Merkel cell carcinoma. *Sci. Rep.* 7:2290. https://doi.org/10.1038/s41598-017-02608-0

Robbins, P.F., Y.C. Lu, M. El-Gamil, Y.F. Li, C. Gross, J. Gartner, J.C. Lin, J.K. Teer, P. Cliften, E. Tycksen, et al. 2013. Mining exomic sequencing data to identify mutated antigens recognized by adoptively transferred tumor-reactive T cells. *Nat. Med.* 19:747–752. https://doi.org/10.1038/nm.3161

Sanjana, N.E., O. Shalem, and F. Zhang. 2014. Improved vectors and genome-wide libraries for CRISPR screening. *Nat. Methods.* 11:783–784. https://doi.org/10.1038/nmeth.3047

Schumacher, T.N., and R.D. Schreiber. 2015. Neoantigens in cancer immunotherapy. *Science.* 348:69–74. https://doi.org/10.1126/science.aaa4971

Setiadi, A.F., M.D. David, R.P. Seipp, J.A. Hartikainen, R. Gopaul, and W.A. Jefferies. 2007. Epigenetic control of the immune escape mechanisms in malignant carcinomas. *Mol. Cell. Biol.* 27:7886–7894. https://doi.org/10.1128/MCB.01547-07

Sette, A., and J. Sidney. 1999. Nine major HLA class I supertypes account for the vast preponderance of HLA-A and -B polymorphism. *Immunogenetics.* 50:201–212. https://doi.org/10.1007/s002510050594

Shin, D.S., J.M. Zaretsky, H. Escuin-Ordinas, A. Garcia-Diaz, S. Hu-Lieskovan, A. Kalbasi, C.S. Grasso, W. Hugo, S. Sandoval, D.Y. Torrejon, et al. 2017. Primary Resistance to PD-1 Blockade Mediated by JAK1/2 Mutations. *Cancer Discov.* 7:188–201. https://doi.org/10.1158/2159-8290.CD-16-1223

Sidney, J., B. Peters, N. Frahm, C. Brander, and A. Sette. 2008. HLA class I supertypes: a revised and updated classification. *BMC Immunol.* 9:1. https://doi.org/10.1186/1471-2172-9-1

Snyder, A., V. Makarov, T. Merghoub, J. Yuan, J.M. Zaretsky, A. Desrichard, L.A. Walsh, M.A. Postow, P. Wong, T.S. Ho, et al. 2014. Genetic basis for clinical response to CTLA-4 blockade in melanoma. *N. Engl. J. Med.* 371:2189–2199. https://doi.org/10.1056/NEJMoa1406498

Snyder, J.T., M.A. Alexander-Miller, J.A. Berzofskyl, and I.M. Belyakov. 2003. Molecular mechanisms and biological significance of CTL avidity. *Curr. HIV Res.* 1:287–294. https://doi.org/10.2174/1570162033485230

Sucker, A., F. Zhao, N. Pieper, C. Heeke, R. Maltaner, N. Stadtler, B. Real, N. Bielefeld, S. Howe, B. Weide, et al. 2017. Acquired IFNγ resistance impairs anti-tumor immunity and gives rise to T-cell-resistant melanoma lesions. *Nat. Commun.* 8:15440. https://doi.org/10.1038/ncomms15440

Tiwari, N., N. Garbi, T. Reinheckel, G. Moldenhauer, G.J. Hämmerling, and F. Momburg. 2007. A transporter associated with antigen-processing independent vacuolar pathway for the MHC class I-mediated presentation of endogenous transmembrane proteins. *J. Immunol.* 178:7932–7942. https://doi.org/10.4049/jimmunol.178.12.7932

Uhlén, M., L. Fagerberg, B.M. Hallström, C. Lindskog, P. Oksvold, A. Mardinoglu, Å. Sivertsson, C. Kampf, E. Sjöstedt, A. Asplund, et al. 2015. Tissue-based map of the human proteome. *Science.* 347:1260419. https://doi.org/10.1126/science.1260419

van der Burg, S.H., M.J. Visseren, R.M. Brandt, W.M. Kast, and C.J. Melief. 1996. Immunogenicity of peptides bound to MHC class I molecules depends on the MHC-peptide complex stability. *J. Immunol.* 156:3308–3314.

van Hall, T., E.Z. Wolpert, P. van Veelen, S. Laban, M. van der Veer, M. Roseboom, S. Bres, P. Grufman, A. de Ru, H. Meiring, et al. 2006. Selective cytotoxic T-lymphocyte targeting of tumor immune escape variants. *Nat. Med.* 12:417–424. https://doi.org/10.1038/nm1381

Viganò, S., D.T. Utzschneider, M. Perreau, G. Pantaleo, D. Zehn, and A. Harari. 2012. Functional avidity: a measure to predict the efficacy of effector T cells? *Clin. Dev. Immunol.* 2012:153863. https://doi.org/10.1155/2012/153863

Wei, M.L., and P. Cresswell. 1992. HLA-A2 molecules in an antigen-processing mutant cell contain signal sequence-derived peptides. *Nature.* 356:443–446. https://doi.org/10.1038/356443a0

Yewdell, J.W., H.L. Snyder, I. Bacik, L.C. Antón, Y. Deng, T.W. Behrens, T. Bachi, and J.R. Bennink. 1998. TAP-independent delivery of antigenic peptides to the endoplasmic reticulum: therapeutic potential and insights into TAP-dependent antigen processing. *J. Immunother.* 21:127–131. https://doi.org/10.1097/00002371-199803000-00006

Zaretsky, J.M., A. Garcia-Diaz, D.S. Shin, H. Escuin-Ordinas, W. Hugo, S. Hu-Lieskovan, D.Y. Torrejon, G. Abril-Rodriguez, S. Sandoval, L. Barthly, et al. 2016. Mutations Associated with Acquired Resistance to PD-1 Blockade in Melanoma. *N. Engl. J. Med.* 375:819–829. https://doi.org/10.1056/NEJMoa1604958

Zitvogel, L., M. Ayyoub, B. Routy, and G. Kroemer. 2016. Microbiome and Anticancer Immunosurveillance. *Cell.* 165:276–287. https://doi.org/10.1016/j.cell.2016.03.001